

## Research Article

# A Formal Model for Performance and Energy Evaluation of Embedded Systems

**Bruno Nogueira,<sup>1,2</sup> Paulo Maciel,<sup>1</sup> Eduardo Tavares,<sup>1</sup> Ermeson Andrade,<sup>1</sup> Ricardo Massa,<sup>1</sup> Gustavo Callou,<sup>1</sup> and Rodolfo Ferraz<sup>1</sup>**

<sup>1</sup>Informatics Center, Federal University of Pernambuco, 50.740-560 Recife, Brazil

<sup>2</sup>Academic Unit of Garanhuns, Federal Rural University of Pernambuco, 55.296-901 Garanhuns, Brazil

Correspondence should be addressed to Bruno Nogueira, bcsn@cin.ufpe.br

Received 2 June 2010; Accepted 21 September 2010

Academic Editor: Dietmar Bruckner

Copyright © 2011 Bruno Nogueira et al. This is an open access article distributed under the Creative Commons Attribution License, which permits unrestricted use, distribution, and reproduction in any medium, provided the original work is properly cited.

Embedded systems designers need to verify their design choices to find the proper platform and software that satisfy a given set of requirements. In this context, it is essential to adopt formal-based techniques to evaluate the impact of design choices on system requirements. To be useful, such techniques must produce accurate results with minimal computation time. This paper proposes an approach based on Coloured Petri Nets for evaluating embedded systems performance and energy consumption. In particular, this work presents a method for specifying and evaluating the workload and the platform components, such as processors and shared or private memories. The method is applied to model single processor and multiprocessor platforms. Experimental results demonstrate an average accuracy of 96% in comparison with the respective measures assessed from the real hardware platform.

## 1. Introduction

The design of embedded systems usually must take into account several nonfunctional constraints, such as performance, size, weight, cost, reliability, and durability. The rapid growth of embedded systems in new application domains introduces new restrictions, which in turn raises new research and technical challenges. One prominent research area is related to battery-operated devices, in which energy consumption plays an important role. The low-power design has grown in importance with the proliferation of such devices. The main challenge is to reduce energy consumption without jeopardizing the performance requirements.

Modern embedded systems are composed of a set of interconnected processing, communication, and storage elements. Very often, these elements are integrated into a single circuit (System-on-Chip). Software (instructions streams/workload) executing on the processing elements drives the behavior of the system. In contrast to a desktop system, which executes a variety of workloads, normally

embedded systems execute only one workload, repeatedly. The characteristics of the workload and the processing elements dictate the usage of communication and storage elements. In turn, the characteristics of the communication and storage elements influence the rate at which the workload is executed. Therefore, energy consumption and performance are a function of the characteristics of the workload and the architectural elements, and thus, estimating these metrics is not an ordinary task.

Given the wide range of platform options and software optimizations, designers need to verify their design choices to find the proper platform and software that satisfy a given set of requirements. Measurement of the actual performance and energy consumption characteristics on real hardware is often not feasible, since this would require the construction of a large number of hardware prototypes. In this context, many model-based approaches for estimating energy consumption and performance have been developed over the last years (e.g., [1–4]). Some of these model the energy consumption adopting cycle-level simulators (also known as

architecture level model approach) [2, 5]. Despite providing very accurate estimates, the low abstraction level adopted by current approaches demands an enormous computational effort, which restricts the applicability for large codes.

This work presents a discrete event modeling strategy, based on Coloured Petri Net formalism (CPN) [6], for performance and energy consumption evaluation of embedded systems using the architecture level model approach. In particular, this paper presents a novel method for specifying and evaluating the performance and energy consumption of embedded systems considering different configurations for workload and the platform components, such as processors and memories. The method is applied to model a real platform, namely, NXP LPC2106, and a theoretical multiprocessor platform. The high level of abstraction of the proposed models allows for fast but accurate estimates. Additionally, although specific platforms have been considered, the modeling approach can be easily applied to other architectures.

Petri Nets (PNs) [7] are well suited to model computer architectures, since both parallelism and conflict, two important characteristics present in modern computer systems, are easily modeled using this formalism. Besides, PN extensions, such as CPN, have proven to be a powerful technique to evaluate performance indices in computer systems [8].

This paper is organized as follows. Section 2 presents related work. Section 3 introduces the required concepts for a better understating of this work. Section 4 presents the proposed approach. Section 5 presents some experiments and Section 6 concludes the paper.

## 2. Related Work

Many approaches have been conceived to model energy consumption in embedded systems. However, few consider multiprocessor architectures. The approaches can be generally classified into two main categories: (i) architecture level (or hardware level) models and (ii) instruction level models. Architecture level models calculate power and energy from detailed descriptions that may comprise circuit level, gate level, and register transfer (RT) level. Instruction level models deal only with instructions and functional units from the software point of view and without knowledge of the underlying hardware organization [9].

The first energy instruction model was introduced in [1, 10]. These works assign an energy cost to each instruction (or sequence of instructions). The cost per instruction is assessed by measuring the average current of the processor when it executes that instruction. Interinstruction effects are also considered. However, the time required to characterize an architecture is a great issue, since the number of measurements grows exponentially with the number of instructions in the Instruction Set Architecture (ISA).

Oliveira et al. [11] proposed a simulation approach based on Coloured Petri Net. That work proposed a stochastic model for the 8051 microcontroller instruction set. The method adopted CPN to model the control flow of a given application and assigned probabilities to conditional branch

instructions, which were translated to CPN transition guard expressions. The main drawback of that strategy is the model complexity, which grows with the application size, hence causing considerable negative impact on simulation time. Such an approach does not allow the evaluation of real-life complex applications or even reasonable size programs. That method was extended in [3] to simplify the model. Although the simulation time is significantly reduced, it is still heavily affected by the code size.

Another instruction level approach, known as functional-level power analysis (FLPA), was introduced in [12] and further extended in [4]. In this method, the processor is separated into functional blocks (such as fetch unit, processing unit, and internal memory). The power consumption of each block is characterized through mathematical functions obtained from several measurements and/or simulations. Thus, the power consumption is obtained by adding up the consumption of all blocks. Although being very fast and having relative good accuracy for estimating power consumption, the proposed analytical modeling presents some limitations for estimating execution time, which in turn affects the energy consumption estimation as shown in their experimental results [4].

Since existing approaches work at a very low level of abstraction (e.g., [2, 5]), architecture level models are known to be very time consuming. Besides, those approaches also need a low-level representation (such as RTL level) of the architecture to allow the power characterization. However, these details of implementation are rarely available for most commercial processors.

## 3. Modeling Formalisms

A stochastic discrete event system (SDES) [13] is a system which occupies a single state for some duration of time, after which an atomic event causes an instantaneous state transition to occur. They are called discrete event systems because their state does not change between subsequent events, whereas state changes occur continuously in a continuous event system. In SDES, stochastic delays (described by probability distribution functions) and probabilistic choices [13] are used to model uncertainties in the system, which may be introduced by many factors such as unpredictable human actions and machine failures. Many SDES models have been developed, for instance, stochastic automata, queuing models, and stochastic Petri nets. In this work, Coloured Petri Nets (CPNs) and Discrete Time Markov Chains (DTMCs) are adopted to model, respectively, the platform and the workload. A comprehensive overview of the modeling possibilities with SDES is out of scope for this paper, but basic concepts are sketched. A much more thorough description of SDES is available in [13–15].

**3.1. Discrete Time Markov Chains.** A Discrete Time Markov Chain  $\{X_t\}$  can be defined as a sequence of random variables  $X_0, X_1, X_2, \dots, X_k$  in which each one of them takes a discrete number of possible values, and where  $t$  is defined over a discrete set. The value taken by  $X_t$  is referred to as the state

of the DTMC at time  $t$ . Following the Markov property, at any  $t = 0, 1, 2, \dots, k$  the conditional probability distribution of the random variable  $X_k$  given the values of its predecessors  $X_0, X_1, \dots, X_{k-1}$  depends only on the value of its immediate predecessor  $X_{k-1}$  but not on the values of  $X_0, X_1, \dots, X_{k-2}$ . Thus, this property states that

$$\begin{aligned} \Pr(X_k = x_k \mid X_0 = x_0, X_1 = x_1, \dots, X_{k-1} = x_{k-1}) \\ = \Pr(X_k = x_k \mid X_{k-1} = x_{k-1}). \end{aligned} \quad (1)$$

A DTMC is said to be time homogeneous, if  $\Pr(X_{k+1} = j \mid X_k = i)$  is independent of  $k$ . In this work, we consider only time homogeneous DTMCs.

Associated with a DTMC is a matrix called the one-step probability transition matrix, denoted by  $P$ , whose  $(i; j)$ th element is given by the probability  $p_{ij}$  of a state transition from state  $X_k = i$  to  $X_{k+1} = j$  in a single step ( $p_{ij} = \Pr[X_{k+1} = j \mid X_k = i]$ ):

$$P = \begin{pmatrix} p_{11} & p_{12} & \cdots & p_{1n} \\ p_{21} & p_{22} & \cdots & p_{2n} \\ \vdots & \vdots & \ddots & \vdots \\ p_{n1} & p_{n2} & \cdots & p_{nn} \end{pmatrix}, \quad (2)$$

$$0 \leq p_{ij} \leq 1, \quad \sum_{j=1}^n p_{ij} = 1 \text{ for each } i.$$

DTMCs can be represented by a directed graph, known as the state-transition diagram. The nodes represent the states of the DTMC and the edges, the transitions between the states labeled by the respective one-step transition probabilities.

The main purpose of establishing a DTMC and the corresponding probability transition matrix  $P$  is to obtain the probability for the modeled system to be in a particular state. From the state probabilities, several performance metrics can be obtained. Let  $\pi = (\pi_1, \pi_2, \pi_3, \dots, \pi_n)$  be the unique vector such that  $\pi = \pi P$  and  $\sum_{k=1}^n \pi_k = 1$  with  $\pi_k \geq 0$ . If the DTMC is finite and irreducible, such unique  $\pi$  exists and is called stationary probability vector [16]. More specifically,  $\pi_i$  is proportion of time spent in state  $i$  in the long-run. Moreover, it can be shown that the average number of visits  $v_j$  to state  $j$  between occurrences of state  $i$  is given by

$$v_j = \frac{\pi_j}{\pi_i}. \quad (3)$$

To evaluate DTMC models, the SHARPE tool [17] has been adopted by this work.

**3.2. Coloured Petri Nets.** A CPN [6] is a bipartite-directed graph, consisting of two types of vertices: (i) places (drawn as circles) and (ii) transitions (drawn as bars). Places model the states, and transitions represent the events of the system. In CPN, a transition is able to fire (enabled) when (i) it has one token of the proper type on each of its input arcs, and (ii) the guard (Boolean expression) attached to the transition holds.

An enabled transition can fire and thus remove tokens from its input places and generate tokens for its output places.

The concept of hierarchical design is supported by CPN. The basic idea is to allow the construction of a large model by using a number of smaller models. These small models are called pages and are connected to each other by places called ports. Such places can be input or output types. It is also possible to use time in CPN models. Time is handled by introducing a global clock and allowing each token to carry a time stamp. A token cannot be used unless the value of the clock has passed or is equal to the value of the time stamp. Intuitively, each time stamp indicates the earliest time at which the token may be used.

In order to show some concepts of CPN, a very simple model is depicted in Figure 1(a) which models the first two stages of a generic pipelined processor. The CPN model consists of two components: pipeline flow and pipeline controller. The places *start*, *fetching*, *fd*, *decoding*, and *execute* model the states of the instruction in the pipeline flow. The place *control* models the control of the flow of instructions through the pipeline. Attached to the transitions *f2* and *d2*, there is a delay of 1, which means one clock cycle, that is, the time required to fetch and decode an instruction in this processor. The marking of places *start* and *fetching* consists of one token each, both with value (colour) *undefined* and time stamp 0, meaning that there is one instruction being fetched and the other is waiting to be fetched. Since these instructions have not been decoded yet, they are classified as *undefined* in the model. As can be seen in Figure 1(a), transition *f2* is enabled because there is a token of type *INSTRUCTION* in its input place (*fetching*), and transition *f1* is disabled because there is no token of colour *fetch* in the place *control*. Similar concepts apply to the other disabled transitions.

When the transition *f2* is fired (see Figure 1(b)), a token is removed from place *fetching* and two tokens are created in places *control* and *fd*. The new tokens get a time stamp which is the current time plus one. At this moment, transition *f1* is enabled as well as transition *d1*. The simulation continues as long as enabled transitions can be found. As can be seen, the model structure makes it impossible for two instructions occupy the places *fetching* or *decoding* at the same time. Additionally, the function *dec()* in the arc (*d2*, *execute*) generates instructions and puts them to execute. This function will be explained in more details in Section 4.1.

To assist our modeling we use the tool CPN Tools [18], which is a mature and well-tested tool that supports editing, simulation, and analysis of CPN.

## 4. Modeling Approach

In this section, the proposed method is presented and applied to evaluating software applications running on the NXP LPC2106, an ARM7TDMI-S-based architecture [19].

**4.1. Architecture Modeling.** The LPC2106 has 128 kB of on-chip FLASH and 64 kB of on-chip SRAM. It has an ARM7TDMI-S processor which enables system designers to build embedded devices requiring small size, low power,

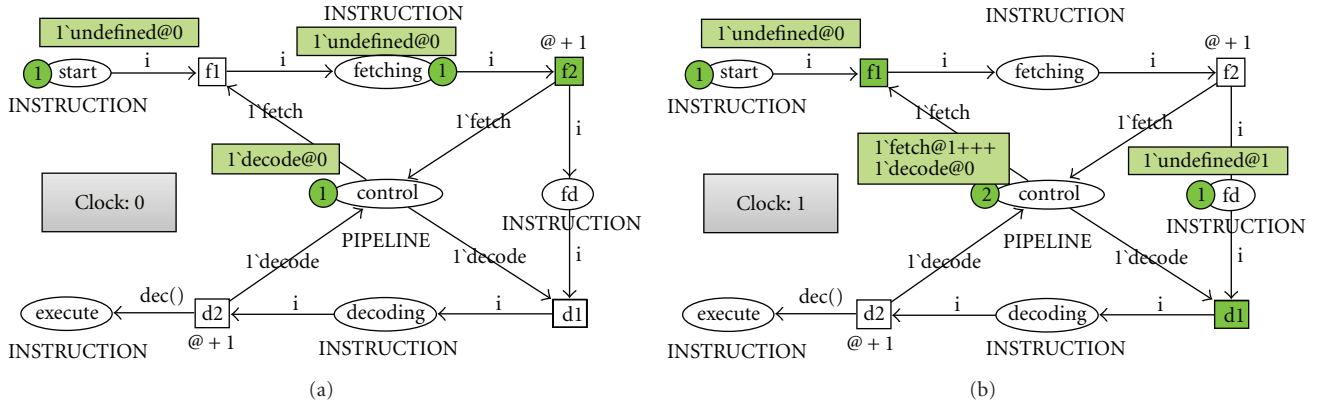


FIGURE 1: CPN model for the first two stages of a pipelined processor.

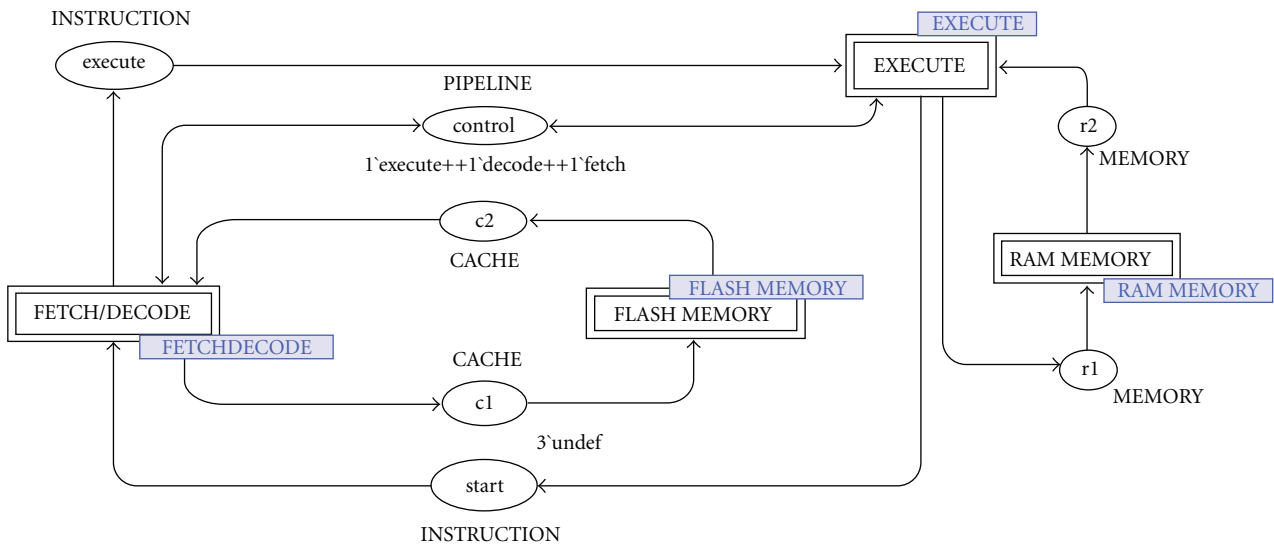


FIGURE 2: CPN model for the LPC2106 architecture (High-level view).

and high performance. Such processor is a 32-bit RISC architecture that consists of a program control unit, an address generator, an integer data path, a general-purpose register bank, and a 3-stage pipeline. An important characteristic of the LPC2106 is an instruction prefetch module, known as Memory Accelerator Module (MAM). The MAM is connected to the local bus and is placed between the FLASH memory and the ARM7TDMI-S core. Like a cache, the MAM attempts to prefetch the next instruction from the FLASH memory in time to prevent CPU fetch stalls.

In order to model the LPC2106 architecture, a library of generic blocks of CPN models has been constructed. These blocks can be combined in a bottom-up manner to model sophisticated behaviors. Modeling a complex architecture thus becomes a relatively simple process. The proposed CPN models are high-level representations that focus on what the architecture should perform instead of on how it is implemented. Moreover, it is important to stress

that once constructed, a building block can be reused in other platform models.

Figure 2 presents the highest-level view of the model, which is composed of the following building blocks (pages, see Section 3.2): *flash memory*, *ram memory*, *fetch/decode*, and *execute*. The *fetch/decode* and *execute* blocks model, respectively, the first two and the last stages of the LPC2106's pipeline. Between these two blocks, there is a place (*control*), which controls the flow of instructions through the pipeline (see Figure 1). The marking of place *control* represents the set of available functional units. The *ram memory* block models the SRAM memory, and the *flash memory* block, the FLASH memory. In these models, timing information is expressed in cycles and is represented through transition firing delays. The energy consumption is expressed in nJ units and is modeled through the *addEnergy* function, which adds the specified energy consumption to the global simulated consumption. Information regarding time and energy consumption was

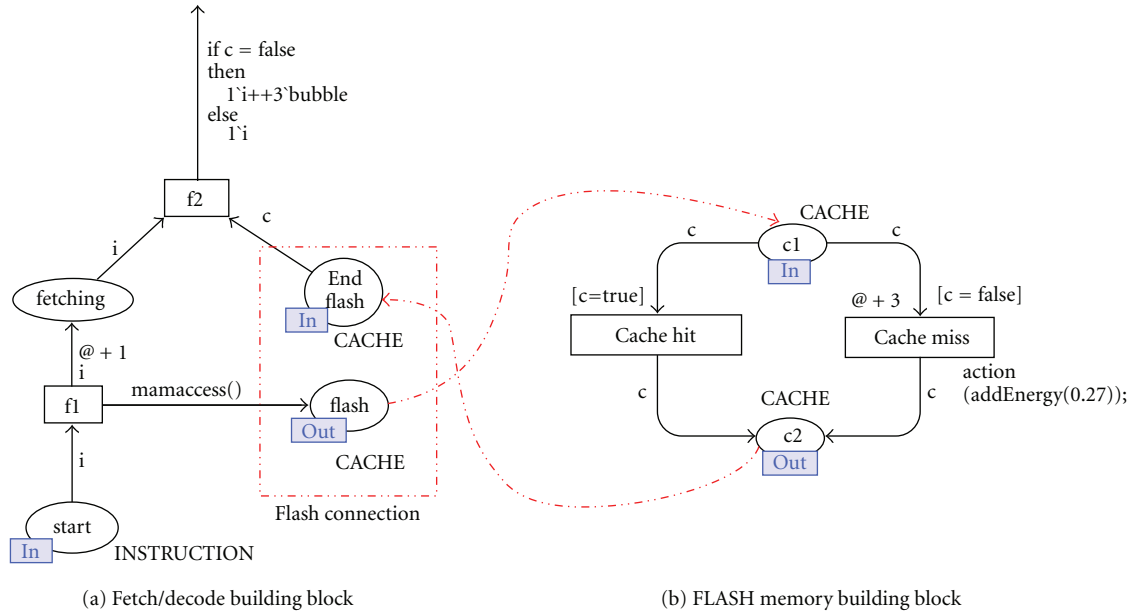


FIGURE 3: Fetch stage and FLASH memory connection.

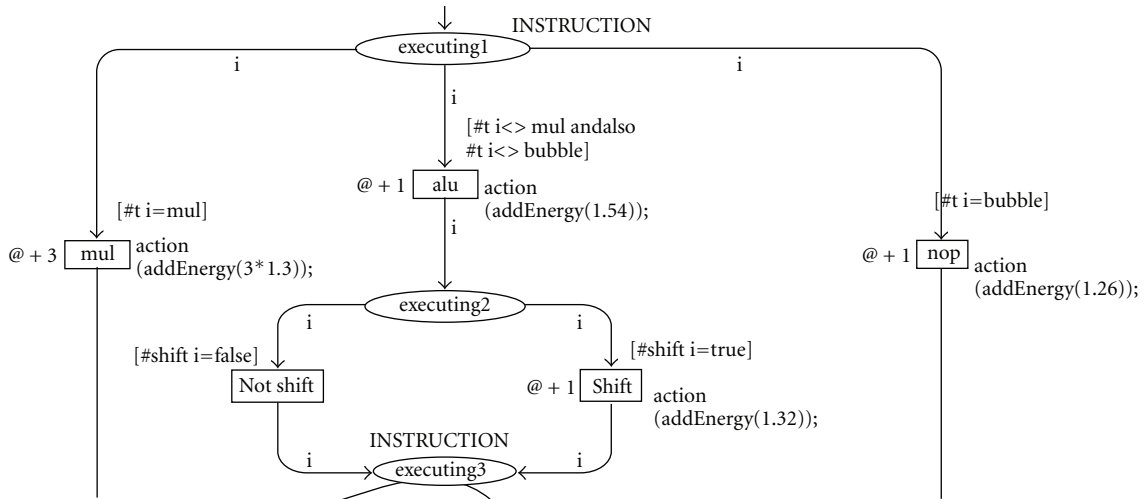


FIGURE 4: Excerpt of the execute building block.

assessed through measurements using the AMALGHMA platform (see Section 4.4) as well as from LPC2106 datasheet [20] and ARM7TDMI-S reference manual [19].

Except for two differences, the *fetch/decode* block is equal to the model presented in Figure 1. Since, in LPC2106 architecture, the FLASH memory stores the application code, the first difference is that the fetch stage is now connected to the *flash memory* block. Figure 3(a) shows this connection and Figure 3(b) shows the *flash memory* block. If the data to be fetched is available in the MAM latches ( $c = true$ ), no flash access is required. Otherwise ( $c = false$ ) one flash access is required and, thus, the respective energy consumption must be computed. The function *mamaccess*

returns a Boolean value. Given the hit ratio of the application under evaluation, firstly it generates a random number with uniform distribution between 0 and 1 and then compares it to the MAM hit ratio. If the random number is less or equal to the hit ratio, this function returns true, or false, otherwise. Accesses to the FLASH memory stall the pipeline, causing the introduction of pipeline bubbles in the wake of the stalled instruction (see the output arc of transition *f2*). The bubbles pass through all stages of the pipeline like any other instruction and then are discarded in the last pipeline stage. The MAM miss ratio must be provided to define the evaluation scenario. To obtain this information, a simple trace-driven simulator was implemented for supporting the

estimation of miss ratios related to specific instruction patterns. This simulator receives as input a trace of the executed instruction addresses and reports the estimated MAM miss ratio.

The second difference is that there are additional transitions in the *fetch/decode* block that are responsible for exchanging the instructions in the fetch and decode stages for bubbles. These transitions become enabled when place *control* receives a token with colour *flush*, generated by the *execute* block when it simulates a branch instruction.

The LPC2106 instruction set has been divided into five classes of instructions according to their performance and energy consumption characteristics: load, store, conditional branch, unconditional branch, data operations, and multiply. For each instruction class, the *execute* block defines the next states and what should be done on the way from one state to another. Figure 4 shows an excerpt of the *execute* block. As can be seen, depending on its class, the instruction may take one of the paths described in the model and the correspondent delay and energy consumption computed. At decode stage, *dec* function (see Figure 1) classifies instructions into one of the instructions classes. This function returns a value of type *INSTRUCTION* in a probabilistic way, such that if an instruction of class *c1* is executed with a frequency of 50% in the code to be evaluated, this function will return an *INSTRUCTION* value of class *c1* with probability of 50%.

**4.2. Workload Specification.** As stated earlier, the *dec* function generates instructions according to the frequency in which each instruction class is executed in the application under evaluation. Since this frequency distribution is dependent on a given software and input data, we devised a method for capturing this information. The method consists in mapping the application code (with annotations) into a DTMC. More specifically, the Control Flow Graph (CFG) of the application is mapped into an irreducible DTMC.

Each basic block  $B_i$  in the CFG is mapped into a state  $X_i$  in the DTMC. Similarly, control flow edges are mapped as transitions between states and are labeled by the state transition probabilities, as

$$P(B_i, B_j) = \Pr(B_i \text{ jumps to } B_j), \quad (4)$$

which defines the probability of executing  $B_j$  after  $B_i$ . Such probabilities are obtained from annotations in the application code.

Figure 5(a) shows an example of code, in which annotations are comments. In this example, the annotation at line 4 indicates that the expression  $x < 10$  evaluates to true with a probability of 50%. The annotation at line 6 indicates that the iterative structure is executed 9 times. The values for the annotations may be captured, for instance, from (i) *ad hoc* designer knowledge, (ii) a more abstract system model, and/or (iii) extensive profiling. Several execution scenarios can be evaluated by simply changing these values. Figure 5(b) depicts the resulting DTMC, where the reader should note an additional transition from state 5 to state 1 (i.e., from the

final to the starting point of the application), which is added to make the DTMC irreducible.

The objective in such a mapping is to compute the average number of times each basic block in the CFG executes (visiting number). Given the stationary probability vector  $\pi = (\pi_1, \pi_2, \dots, \pi_k)$  of the mapped DTMC, which is obtained numerically by the SHARPE tool, let  $v = (v_1, v_2, \dots, v_k)$  be the vector with the average number of executions of each basic block  $B_1, B_2, \dots, B_k$ , where  $B_k$  contains the ending point of the application. Then,  $v$  is determined by (see (3))

$$v = \left( \frac{\pi_1}{\pi_k}, \frac{\pi_2}{\pi_k}, \dots, \frac{\pi_k}{\pi_k} \right). \quad (5)$$

Given the average number each basic block executes, the frequency in which each instruction is executed can be obtained, and hence the execution frequency of each class.

The methodology flow for the estimation of the energy consumption and execution time in an architecture for a given application is shown in Figure 6. The architectural model is constructed by the composition of CPN building blocks (right side of Figure 6). The building blocks represent functional units of the architecture under evaluation and are modeled in a high abstraction level, allowing flexibility, reuse, and rapid evaluation. These building blocks are annotated with values regarding energy consumption (*addEnergy* function) and performance (CPN delays) of the modeled functional unit. Next, the code which will execute on the embedded platform is mapped on the architectural model by a compiler (see Section 4.5). Finally, the model evaluation is made by means of stochastic simulation (Section 4.3).

**4.3. Evaluation.** The evaluation is made by means of simulation. The facilities of CPN Tools have been adopted to define analysis functions and to perform data collection. Basically, two performance metrics were defined: (i) the average execution time per instruction and (ii) the average energy consumption per instruction. Given these metrics and the number of executed instructions in the application and the processor's operating frequency, the overall energy consumption and execution time of an application is obtained.

Firstly, a *breakpoint monitor* [8] was defined and assigned to the last transition in the *execute* block. This transition is always fired by all instruction classes. The *breakpoint monitor* collects data and tests if the metrics satisfy the stop criterion. If so, the simulation stops; otherwise, the simulation continues. To calculate the metrics, two data are collected on the firing of the transition linked with the *breakpoint monitor*: (i) the interval firing time, that is, the current time minus the last firing time, and (ii) the interval energy consumption, that is, the current global energy consumption minus the global energy consumption of the last firing. We designed a set of statistical functions so that a confidence interval for the metrics could be constructed. The stop criterion defines that if the confidence interval of these two metrics satisfies the specified precision, the simulation stops. The precision is specified by two parameters: (i) the confidence level and (ii) the relative error. This work adopted

TABLE 1: Experimental results.

	Execution Time ( $\mu$ s)			Energy Consumption ( $\mu$ J)		
	Estimated	Measured	Error	Estimated	Measured	Error
adpcm	12397.3	13080.1	5.22%	1065.77	1097.28	2.87%
bcnt	55.2	56.1	1.60%	4.62	4.63	0.22%
binary search	5.9	5.8	1.72%	0.49	0.50	2%
bubble sort	6162.3	6138.3	0.39%	5189.8	5247.6	1.10%
convolution	964.9	1076.9	10.2%	76.9	80.1	4%
fdct	90.9	93.4	2.68%	7.83	8.21	4.63%
oximeter (1)	11.6	11.9	2.52%	0.99	1.01	1.98%
oximeter (2)	11.7	12.3	5.26%	0.99	1.07	7.48%
oximeter (3)	3357.2	3379	0.65%	283.05	257.21	10.02%

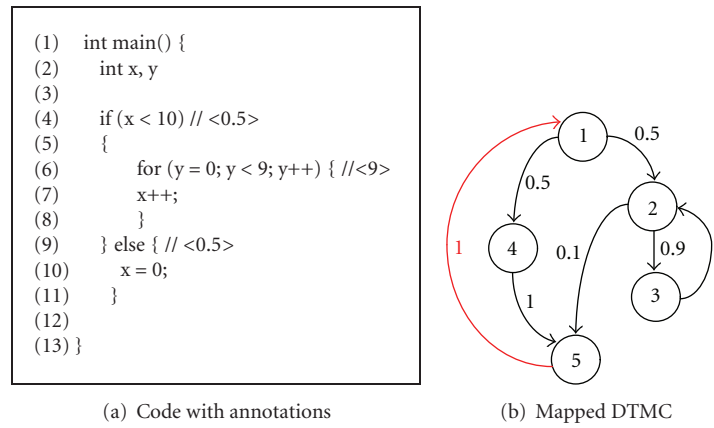


FIGURE 5: Code mapping example.

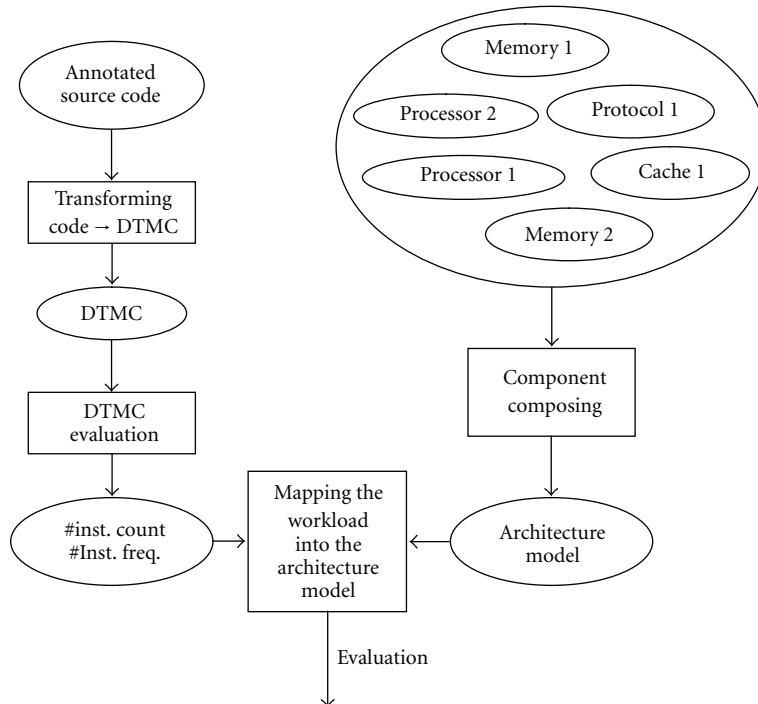


FIGURE 6: Proposed methodology flow.

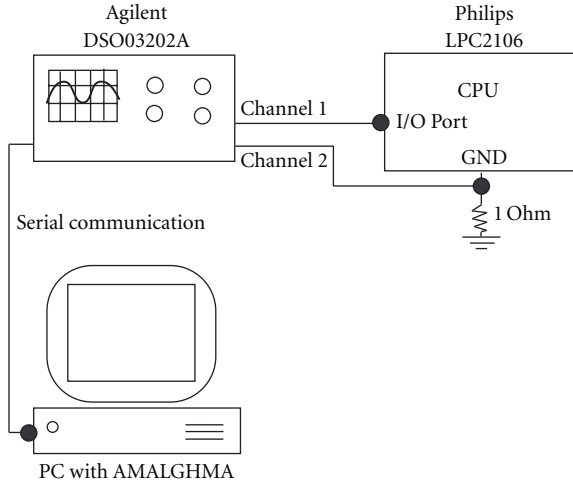


FIGURE 7: Measurement scheme.

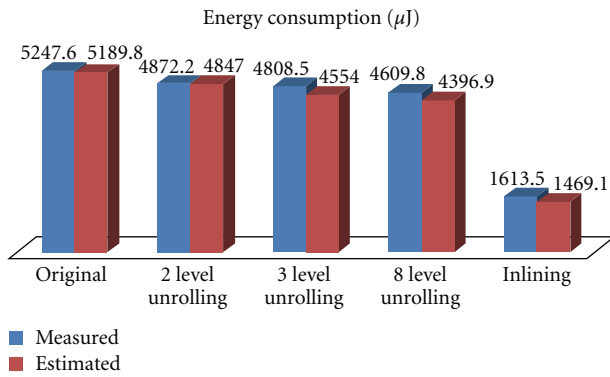


FIGURE 8: Code optimizations.

TABLE 2: Simulation time comparison.

	A1 (s)	A2 (s)
Task 1	2	4
Task 2	2	3
Task 3	1085	2

a confidence level of 95% and a maximum relative error of 2%.

**4.4. Measuring Strategy.** This section describes the measuring method adopted to obtain the energy consumption and execution time values employed in the proposed models. To capture the average energy consumption of each functional unit defined in the model, assembly codes that stimulate, separately, the respective functional unit of the LPC2106 have been implemented, uploaded on the platform, executed, measured, and then the obtained data were statistically analyzed. For example, to capture the average power consumption when a MAM miss occurs, an assembly code that forces MAM misses was designed.

```

(1) void BubbleSort (int Array[])
(2) {
(3)     int i, j;
(4)     int k = NUMELEMENS-1;
(5)
(6)     for (I = 0; i < NUMELEMENS; i++) // <100>
(7)     {
(8)         for (j = 0; j < k; j = j + 1) // <4950>
(9)         {
(10)            if (Array[j] > Array[j + 1]) // <0.5>
(11)            {
(12)                swap(Array, j, j + 1);
(13)            }
(14)        }
(15)        k--;
(16)    }
(17) }

```

FIGURE 9: Bubblesort algorithm.

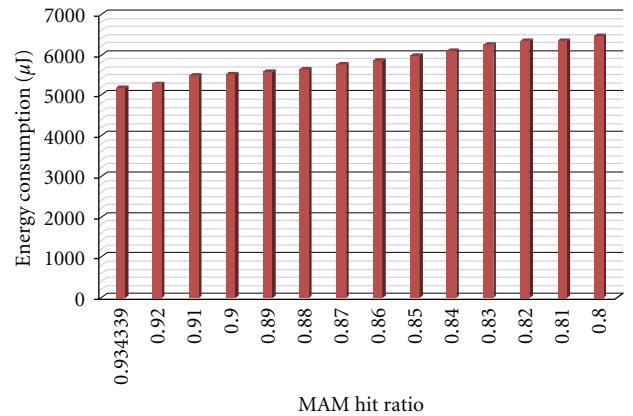


FIGURE 10: Bubblesort: energy consumption in function of the MAM hit rate variations.

The AMALGHMA (Advanced Measurement Algorithms for Hardware Architectures) tool has been implemented for automating the measuring activities. AMALGHMA adopts a set of statistical methods, such as bootstrap and parametric methods, which are important in the measurement process due to several factors, for instance, (i) oscilloscope resolution and (ii) resistor error. Besides, the results estimated by AMALGHMA were compared and validated considering LPC2106 datasheet as well as ARM7TDMI-S reference manual.

The measurement scheme is shown in Figure 7. To measure power consumption, a workstation executing the AMALGHMA tool is connected to an Agilent DSO03202A oscilloscope, which captures the platform-drained current by measuring the voltage drop across a 1 Ohm sense resistor (average microcontroller impedance is order of magnitude higher than this). The oscilloscope is also connected to an I/O port of the LPC2106, which is used to monitor the code's starting and end times. Given this, the code's execution time is also estimated. Even for very short duration software functions, the AMALGHMA tool is able to estimate

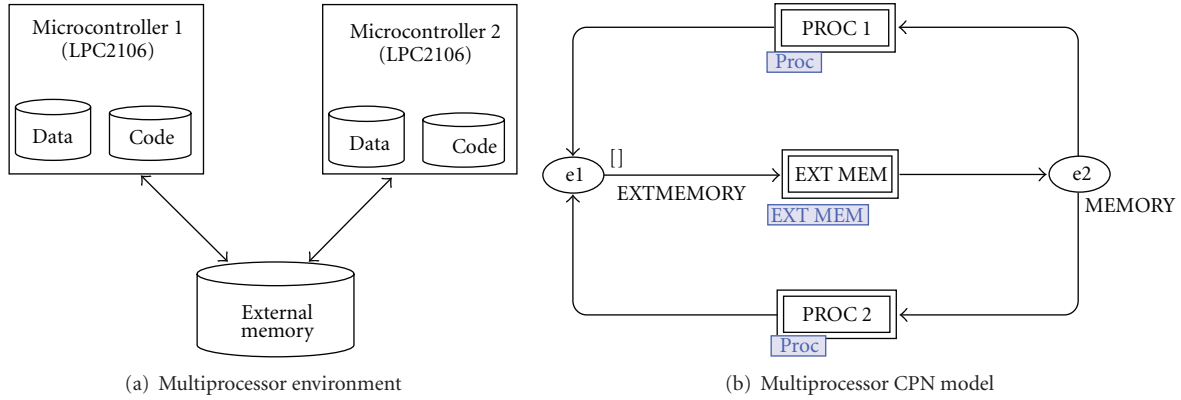


FIGURE 11: Multiprocessor case study.

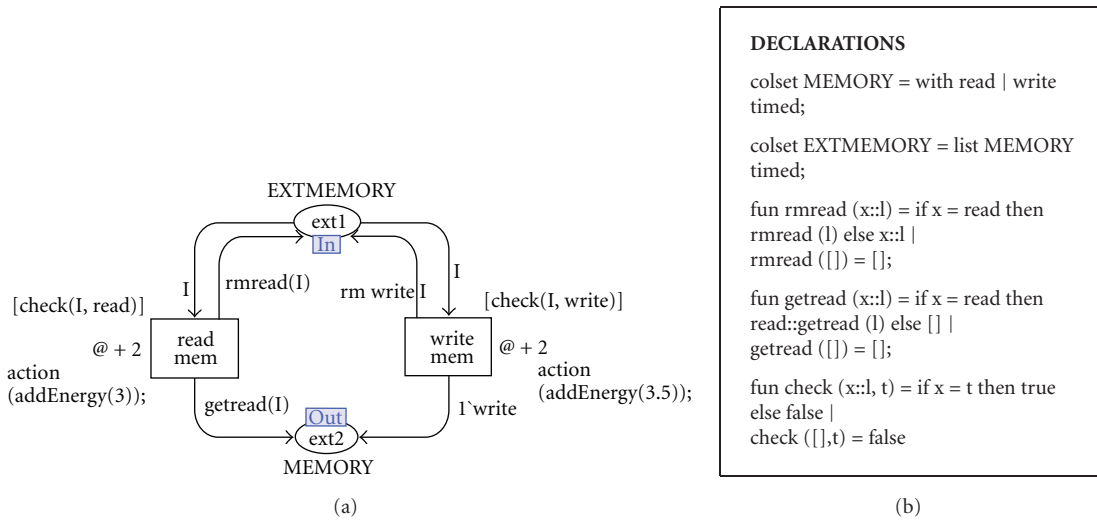


FIGURE 12: External memory model.

the average execution time, its energy consumption, and other related statistics. For doing that, sampling and statistics strategies have been implemented [21].

**4.5. PECES Tool.** An additional contribution of this work was the development of a computational tool to automate same steps of the proposed methodology. The tool was named PECES (Performance and Energy Consumption Evaluation of Embedded Systems). It receives the annotated source code and the architecture model as input and returns the average execution time and energy consumption as output.

The following steps are performed by PECES to evaluate a code.

- (1) It compiles the application source code using the option to generate intermediate assembly code. GCC (arm-uclibc-gcc [22]) has been adopted as compiler.
- (2) PECES builds the Control Flow Graph (CFG) using the intermediate code generated in the previous step.

- (3) It uses the CFG and the annotations from the source code to generate the corresponding irreducible DTMC.
- (4) The DTMC is numerically evaluated in SHARPE, so as to obtain the stationary probabilities.
- (5) It uses the stationary probabilities to calculate the average number of execution for each basic block and, then, the number of times each instruction is executed. Next, PECES clusters instructions from the same class and calculates the frequency each class executes.
- (6) The distribution frequency is written in the architecture model.
- (7) PECES invokes Access/CPN tool [23] to simulate the architecture model.
- (8) Finally, the tool uses the average execution time per instruction and the average energy consumption per instruction obtained from the previous step to calculate the average execution time and the energy consumption.

## 5. Experimental Results

This work has conducted some case studies to evaluate the proposed estimation methods. The case studies consist of (i) Motorola's Powerstone benchmark suite codes (adpcm, bcnt, and fdct), (ii) common search/ordering/signal processing algorithms (binarysearch, bubblesort, and convolution), (iii) a customized example, and (iv) a real-world biomedical application (a pulse oximeter). The pulse oximeter case study is composed of three concurrent tasks; hence it has been divided into three separate experiments. All experiments were performed on an Intel Core 2 Duo 1.67 GHz, 2 Gb RAM, and Windows Vista OS.

Table 1 shows the estimated energy consumption and execution time compared to the measured values for the case studies. The comparison yields an average error of 3.36% and maximum error of 10.2% for the estimated execution time. Regarding the energy consumption, the average error was of 3.81% with maximum of 10.02%.

The pulse oximeter experiment was adopted to compare the simulation time of the proposed approach against the instruction-simulation method presented in [3], which also modeled the LPC2106 (although the MAM has not been considered) and reported an average error of 4% for the estimated metrics. Table 2 depicts quantitative results, in which A2 represents the proposed approach, and A1 represents the approach presented in [3]. Results in A2 also include the time to generate and evaluate the DTMCs, which took less than one second for all codes. Results show that the simulation time in both methods are almost the same, except for the third task. In this task, the proposed approach was 542 times faster. The huge difference is mainly because [3] simulates the control flow of the application; hence, the simulation model and the simulation time grow with the code size. On the other hand, in the method proposed by this work, the model has a fixed size; the variations occur only on the frequency in which each instruction class is executed.

**5.1. Applications of the Method.** Code optimizations, such as loop unrolling and function inlining, have proven to be successful techniques to improve the system performance. A very useful application for the proposed method is to verify the effect of these common code optimizations on system energy consumption. The bubblesort experiment has been used to demonstrate how such what-if analysis may be carried out.

The bubblesort code was optimized in four steps. From step to step more aggressive optimizations have been included. Figure 8 shows the results of this experiment. It can be seen that by applying such optimizations the energy consumption was optimized in 225%. The average error for the estimated values was of 4.38%, showing that the proposed method may be successfully employed for performing energy aware code optimizations.

The proposed method is also useful when it comes to evaluating code operation scenarios, such as best-case, average-case, and worst-case scenarios. The bubblesort code has been used to evaluate such application.

The bubblesort code is depicted in Figure 9, where the reader should note that all code flow variance is defined by the three structures at lines 6, 8, and 10. The iteration number at lines 6 and 8 is array-length dependent, in which a deterministic behavior is performed. On the other hand, the control structure at line 10 has a probabilistic behavior, depending on the ordering level of the array. In the worst-case scenario, the array is fully unordered; hence the function *swap* will be called every time. Such scenario may be evaluated by setting the annotation value at line 10 to 1. The best-case scenario happens when the array is fully ordered. In this case, the function *swap* will never be called. By simply setting the annotation value at line 10 to 0, this scenario may be evaluated. On the other hand, the average-case scenario happens when the array is partially ordered. Such scenario may also be evaluated by setting the annotation value at line 10 to 0.5. Table 3 shows the results for each scenario. The estimated values for the execution time yield an average error of 1.69% and maximum error of 3.94%. Regarding the energy consumption, the average error was of 2.34% with maximum of 5.24%.

As stated earlier, the MAM hit rate must be given in order to allow accurate evaluations. Nevertheless, meaningful results may also be obtained if we consider the energy consumption (or the execution time) in function of the MAM hit rate variations. Figure 10 shows the estimated energy consumption of the bubblesort code in function of the MAM hit rate variations, where it can be seen that the energy consumption increases when the MAM hit rate decreases.

**5.2. Modeling Multiprocessors Architectures.** In what follows, we present how the CPN basic models can be used to represent and evaluate more complex system architectures. In particular, this section presents a shared memory multiprocessor architecture, in which each microcontroller has its own MAM latches (acting as very small cache devices). Hence, this case study presents a study of a hierarchical shared memory multiprocessor architecture, where each microcontroller has a three-phase pipeline. Thus, consider a hardware platform with two LPC2106 sharing an external memory (see Figure 11(a)). The external memory interface can only sustain one write access every two cycles, whereas no such limitation exists for read accesses. Incoming requests are placed in a queue and processed in a First In-First Out policy. It is important to remember that each LPC2106 is also connected to two private memories containing program code and data.

The hardware platform described above was modeled by replicating the model already presented for the LPC2106 and creating a new building block to represent the external memory. Figure 11(b) depicts the proposed model for this environment, and Figure 12 presents the external memory model. Figure 12 also presents the CPN declarations for the external memory. Incoming requests to the external memory are placed in a queue in *e1* (Figure 11(b)). Transitions *read mem* or *write mem* (see Figure 12) become enabled whenever there are incoming requests in the queue of place *ext1*.

TABLE 3: Bubblesort typical scenarios results.

	Execution Time ( $\mu$ s)			Energy Consumption ( $\mu$ J)		
	Estimated	Measured	Error	Estimated	Measured	Error
best-case	2414.6	2432,5	0.74%	2028.9	2015.6	0.66%
average-case	4086.6	4247,8	3.94%	3453.4	3634.4	5.24%
worst-case	6162.3	6138.3	0.39%	5189.8	5247.6	1.11%

TABLE 4: Multiprocessor evaluation results.

	Evaluation time (s)	Energy consumption ( $\mu$ J)	Execution time ( $\mu$ s)
one adpcm (one microcontroller)	6	1065.77	12397.3
two adpcms (two microcontrollers)	17	2408.5	13118.4

When *read mem* or *write mem* is fired, the correspondent energy consumption and delay are computed.

This model was evaluated using the adpcm experiment, where one adpcm code runs on each microcontroller. We also assumed that 30% of the memory instructions access the external memory. Table 4 shows the results (line 2) of this experiment as well as the results (line 1) regarding the execution of one adpcm in just one microcontroller (already show in Table 1). Comparing the two results, the energy consumption almost doubled, since besides the energy consumption of the external memory, two processors consume more energy than just one. On the other hand, the execution time remained almost the same. Actually, since the external memory introduces a bottleneck, there is a slightly increase in this value. However, as in line 1 just one adpcm is running, the reader should note the execution time improvement in the parallel execution of two adpcms codes in comparison to the sequential execution of these codes.

## 6. Conclusions

This work presented a method for evaluating energy consumption and performance in embedded systems. The proposed method adopts Coloured Petri Nets for modeling the functional behavior of processors and memory architectures at a high-level of abstraction. Further, the workload under evaluation is mapped into the hardware model to carry out the performance and energy consumption estimation. A tool, named PECES, was implemented for automatizing the method. Additionally, a measuring platform, named AMAL-GHMA, was constructed for characterizing the platform and for comparing the respective results provided by the proposed method.

This work adopted a real-world embedded platform as case study, and the experimental results show that the proposed approach may be used to ensure a rapid and reliable feedback to the designer. Besides, applications of the method, such as the modeling of multiprocessor architectures, were demonstrated. As future work, we plan to improve PECES

for helping the designer in the platform model construction and to validate the method in other architectures.

## References

- [1] V. Tiwari, S. Malik, and A. Wolfe, "Power analysis of embedded software: a first step towards software power minimization," *IEEE Transactions on Very Large Scale Integration (VLSI) Systems*, vol. 2, no. 4, pp. 437–445, 1994.
- [2] D. Brooks, V. Tiwari, and M. Martonosi, "Wattch: a framework for architectural-level power analysis and optimizations," in *Proceedings of the 27th Annual International Symposium on Computer Architecture (ISCA '07)*, pp. 83–94, June 2000.
- [3] G. de Almeida Callou, P. Maciel, E. de Andrade, B. Nogueira, and E. Tavares, "A coloured petri net based approach for estimating execution time and energy consumption in embedded systems," in *Proceedings of the 21st Annual Symposium on Integrated Circuits and System Design*, pp. 134–139, 2008.
- [4] E. Senn, J. Laurent, N. Julien, and E. Martin, "Algorithmic level power and energy optimization for DSP applications: SoftExplorer," in *Proceedings of the IEEE International Symposium on Image/Video Communications (ISIVC '04)*, 2004.
- [5] W. Ye, N. Vijaykrishnan, M. Kandemir, and M. J. Irwin, "The design and use of SimplePower: a cycle-accurate energy estimation tool," in *Proceedings of the 37th Design Automation Conference (DAC '00)*, pp. 340–345, June 2000.
- [6] K. Jensen, *Coloured Petri Nets: Basic Concepts, Analysis Methods, and Practical Use*, Springer, New York, NY, USA, 1992.
- [7] T. Murata, "Petri nets: properties, analysis and applications," *Proceedings of the IEEE*, vol. 77, no. 4, pp. 541–580, 1989.
- [8] L. Wells, *Performance analysis using coloured petri nets*, Ph.D. thesis, University of Aarhus, July 2002.
- [9] C. Bleakley, M. Casas-Sanchez, and J. Rizo-Morente, "Software level power consumption models and power saving techniques for embedded DSP processors," *Journal of Low Power Electronics*, vol. 2, no. 2, pp. 281–290, 2006.
- [10] V. Tiwari and M. T.-C. Lee, "Power analysis of a 32-bit embedded microcontroller," *VLSI Design*, vol. 7, no. 3, pp. 225–242, 1998.
- [11] M. N. Oliveira Jr., S. Neto, P. Maciel et al., "Analyzing software performance and energy consumption of embedded systems by probabilistic modeling: an approach based on coloured petri nets," in *Proceedings of the 27th International Conference on Applications and Theory of Petri Nets and Other Models of Concurrency (ICATPN '06)*, vol. 4024 of *Lecture Notes in Computer Science*, pp. 261–281, 2006.
- [12] J. Laurent, E. Senn, N. Julien, and E. Martin, "High-level energy estimation for DSP systems," in *Proceedings of the International Workshop on Power and Timing Modeling, Optimization and Simulation (PATMOS '01)*, pp. 311–316, Yverdon-Les-Bains, Switzerland, September 2001.
- [13] A. Zimmermann, *Stochastic Discrete Event Systems: Modeling, Evaluation, Applications*, Springer, New York, NY, USA, 2007.

- [14] C. Cassandras and S. Lafortune, *Introduction to Discrete Event Systems*, Springer, New York, NY, USA, 2008.
- [15] G. Bolch, S. Greiner, H. de Meer, and K. Trivedi, *Queueing Networks and Markov Chains*, Wiley-Interscience, New York, NY, USA, 2005.
- [16] W. Stewart, *Probability, Markov Chains, Queues, and Simulation: The Mathematical Basis of Performance Modeling*, Princeton University, Princeton, NJ, USA, 2009.
- [17] C. Hirel, R. Sahner, X. Zang, and K. Trivedi, "Reliability and performability modeling using sharpe," in *Proceedings of the 11th International Conference on Computer Performance Evaluation. Modelling Techniques and Tools*, vol. 1786 of *Lecture Notes in Computer Science*, pp. 345–349, Schaumburg, Ill, USA, March 2000.
- [18] A. Vinter Ratzler, L. Wells, H. Lassen et al., "CPN tools for editing, simulating, and analysing coloured petri nets," in *Proceedings of the 24th International Conference on Applications and Theory of Petri Nets*, vol. 2679 of *Lecture Notes in Computer Science*, pp. 450–462, Springer, Eindhoven, The Netherlands, 2003.
- [19] ARM Limited, "ARM7TDMI-S Technical Reference Manual (Rev. 4)," 2001.
- [20] Philips Electronics, "NXP LPC2104, LPC2105, LPC2106 Data Sheet," 2004.
- [21] D. Lilja, *Measuring Computer Performance: A Practitioner's Guide*, Cambridge University Press, Cambridge, UK, 2005.
- [22] Keil, "Gcc compiler," <https://www.keil.com/demo/eval/arm.htm>.
- [23] M. Westergaard and L. Kristensen, "The access/CPN framework: a tool for interacting with the CPN tools simulator," in *Proceedings of the 30th International Conference on Applications and Theory of Petri Nets*, vol. 5606 of *Lecture Notes in Computer Science*, pp. 313–322, Springer, 2009.